

Hydrophobic Modification of Cellulose Nanocrystals from Bamboo Shoots Using Rarasaponins

Christian J. Wijaya, Suryadi Ismadji, Hakun W. Aparamarta, and Setiyo Gunawan*



Cite This: *ACS Omega* 2020, 5, 20967–20975



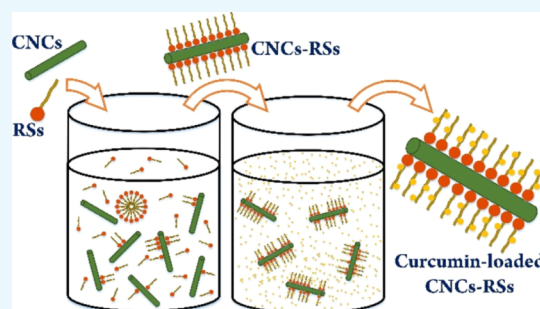
Read Online

ACCESS |

Metrics & More

Article Recommendations

ABSTRACT: Because of their hydrophilic tendencies, the modification of cellulose nanocrystals (CNCs) is needed for applying them as a hydrophobic drug carrier. Previous studies have investigated several modification agents, such as cetyltrimethylammonium bromide. Natural surfactants, such as rarasaponins (RSs), are suitable to avoid human health and environmental issues. In this work, RSs were attached onto CNCs from bamboo shoots to enhance their hydrophobicity. The initial RS concentration and the operating temperature were studied to obtain the best conditions for the modification process, which had significances (p -value < 5%) toward the amount of RSs linked on the CNCs (q) as the response. A q as high as 203.81 ± 0.98 mg/g was obtained at an initial RS concentration of 2000 mg/L and an operating temperature of 30 °C. The curcumin uptake on CNCs-RSs reached $12.40 \pm 0.24\%$, while it was slowly released until approximately 78% in 3 days.



1. INTRODUCTION

As an advanced cellulose-based nanomaterial, cellulose nanocrystals (CNCs) can be applied in several applications. One promising application of CNCs is as a drug carrier in a drug-delivery system. These are applicable because of their marvelous characteristics, such as biodegradability, biocompatibility, low cytotoxicity, and excellent thermal stability.^{1,2} Besides that, CNCs come from the most abundant natural resource (cellulose). The most important thing is that CNCs can be easily modified to overcome their limitations,³ such as low loading capacity, hydrophilic tendencies, and poor emulsification performance.^{1,4,5} Based on these characteristics, CNCs are more suitable for carrying hydrophilic drugs. CNCs have been applied as a drug carrier for several hydrophilic drugs, such as ibuprofen,⁶ vit-B₁₂,⁷ tetracycline,⁸ doxorubicin,⁹ hydroquinone,¹⁰ and theophylline.¹¹ Another form of CNCs, such as tunicate CNCs (TCNCs), actually has more advanced characteristics in their stability, strength, and large aspect ratio.^{12,13} However, TCNCs have superhydrophilicity which makes them even harder to be applied in hydrophobic drug-delivery systems.¹²

The easily modified characteristic enables the application of CNCs for hydrophobic or poorly water-soluble drug-delivery system. Physical and chemical modification can be used to increase the hydrophobicity of the CNCs using oils, compounds, polymers, and surfactants. Fatty acids,¹⁴ fatty acid methyl ester,¹⁵ and castor oil² have been studied to establish the hydrophobicity of the CNCs. Several compounds such as folic acid,¹⁶ cyclodextrin,¹⁷ and octenyl succinic anhydride¹⁸ have been used for the surface modification of the

CNCs. Previous research studies have modified the CNCs using poly(lactic acid),⁴ poly(DL-lactide-co-glycolide),¹⁹ and chitosan.^{20–23} A surfactant is the easiest modification agent to be applied because of its two side characteristic, hydrophilic and hydrophobic sides. The hydrophilic side can bind with the CNCs, while the hydrophobic side can be used to bind with the hydrophobic or poorly water-soluble drugs. Cetyltrimethylammonium bromide (CTAB)^{1,3,9,24} is one of the surfactants that has been studied as the modification agent. The CTAB-coated CNCs have been studied to carry the hydrophobic drugs, such as etoposide, docetaxel, paclitaxel,⁹ luteolin, luteoloside,¹ and curcumin.³ From these previous studies, CTAB used as the common surfactant can increase the hydrophobicity of the CNCs. It can be used for binding the hydrophobic drugs and then targeting the diseased human cells. However, CTAB can affect the stabilization of the cell that causes cell death because of the interaction between the CTAB and the cell phospholipid.²⁵ Besides that, the environmental issues are one of the problems caused by the use of CTAB.² Therefore, a natural surfactant such as rarasaponins (RSs) can be used to avoid the health and environmental issues from the use of CTAB. RSs can be obtained from the

Received: May 23, 2020

Accepted: July 28, 2020

Published: August 12, 2020



fruit flesh of the *Sapindus rarak De Candole* plant. This fruit flesh is traditionally used to wash pieces of silver jewelry and batik fabrics because of its surfactant content. RSs have the aglycone (triterpenoid or steroid) region that has hydrophobic characteristic and oligosaccharide chain that has rich hydroxyl groups. This natural surfactant has low toxicity because of its poorly absorbed characteristics when digested.²⁶ Its good characteristics give a high potential for using RSs as the modification agent. The previous study had used CNCs-RSs for adsorbing the tetracycline antibiotic.²⁷ The modification of CNCs using RSs occurs through their OH groups on the surface, where the OH groups trigger the formation of hydrogen bindings on the CNCs-RSs as has been explained in the previous study. However, this study just investigated the effects of CNC-to-RS ratio on the synthesis of CNCs-RSs. Moreover, the tetracycline antibiotic used was more hydrophilic²⁸ so that the uptake was quite low compared to the other materials.

In this study, further investigation was carried out to investigate the effects of the combined parameters between the initial RS concentration and the operation temperature used on the synthesis of CNCs-RSs from bamboo shoot (BS)-based CNCs. BSs were chosen as the raw material of the CNC production because of their high cellulose contents as the main constituent of the CNCs. The modification hypothesized that the hydrophobicity enhanced along with the attachment of RSs on the CNC surface. Because of their hydrophobicity, CNC-RSs were tested to load the curcumin drug as the hydrophobic drug.

2. RESULTS AND DISCUSSION

2.1. CNC Isolation from BSs. As the main constituent of CNCs, the cellulose was isolated first from the BSs by removing the lignin and hemicellulose contents using the pretreatment processes. The high cellulose content ($32.96 \pm 0.40\%$) and low lignin content ($10.00 \pm 0.58\%$) provide great potential for BSs as the CNC raw material. The pretreatment processes were used to break down the complex structure of the cellulose, hemicelluloses, and lignin. The hemicelluloses and lignin were fragmented into their monomers and dissolved in the pretreatment solvents, maintaining the high cellulose content. As the final product of the pretreatment processes, the pretreated BSs (PBSs) contained a high cellulose content of $76.85 \pm 1.56\%$ with a low lignin content of $0.95 \pm 0.62\%$. These composition data were determined by the Chesson method.²⁹

The CNC production was carried out under the operating condition where the sulfuric acid concentration was 55 wt % and the temperature was 40 °C. This acid hydrolysis process produced the rod-like CNCs with high-enough crystallinity (CrI = 81.49%). This crystallinity index (CrI) value was high enough compared to the previous studies which produced CNCs with the CrI around 70–90%.^{8,30–32} The sulfuric acid solution hydrolyzed the cellulose in the PBSs by cracking the β -glycosidic bonds of the cellulose chains. The amorphous region of the cellulose was broken down into its monomer (glucose), while the crystalline region that is stronger and more stable was fragmented into the shorter cellulose chains.

2.1.1. RS Extraction from *S. rarak De Candole*. The RSs were extracted using distilled water from the dried fruit flesh of *S. rarak De Candole*. The extraction of RSs is easily performed using a polar solvent, even the RSs can be dissolved in the polar and nonpolar solvent because of its hydrophilic and

hydrophobic characteristic. The average yield of this extraction process was $63.98 \pm 1.36\%$ from three experiment replications. The total saponin content was measured using a UV/Vis spectrophotometer. Here, diosgenin was used as the standard solution because it is the sugar-free product (aglycone region) from the hydrolysis of saponins. For determining the total saponin content, the RS solution was treated using a high concentration of the sulfuric acid solution that would hydrolyze the saponins. The total saponin content obtained in the RS extract was $76.74 \pm 1.46\%$. It is high enough to be used as the modification agent for the CNCs. The crude extract of RSs was directly used for modifying the CNCs without any further purification.

RSs are a natural compound that contains an aglycone chain linked to one or more oligosaccharide moieties. The aglycone chain has a hydrophobic characteristic because of its steroid or triterpenoid group. On the other hand, the oligosaccharide chain has a hydrophilic characteristic because of the rich hydroxyl group. As shown in Figure 1, the hydroxyl groups

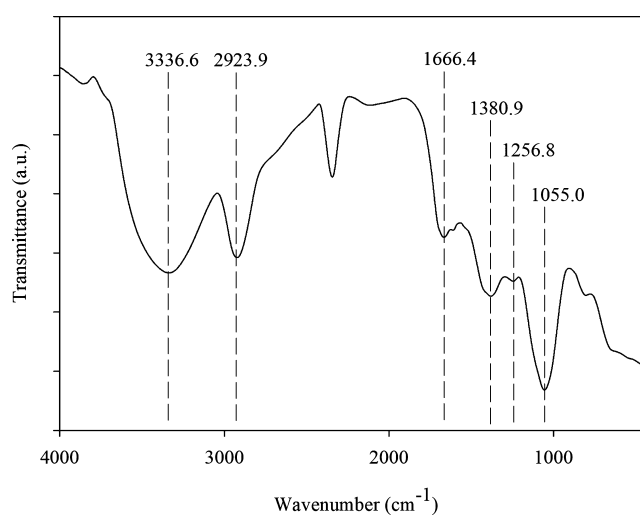


Figure 1. FTIR spectra of RSs.

(OH stretching) and the aromatic ring groups (C=C stretching) are shown at the absorption peaks of 3336.6 and 1055.0 cm^{-1} , respectively. The other peaks at 2923.9, 1666.4, 1380.9, and 1256.8 cm^{-1} indicate the presence of C–H stretching, olefin functional groups, C–H bending vibrations, and C–O stretching (carbonyl groups), respectively.³³

2.2. Surface Modification of CNCs. From the zeta potential analysis, the CNCs provided a zeta potential of -11.0 mV because of their sulfate groups on the CNC surface. The use of sulfuric acid in the acid hydrolysis made several hydroxyl groups substituted by the sulfate groups.³⁴ It presented a negative charge of the CNC surface. The zeta potential of RSs was also analyzed for investigating the binding of CNCs and RSs in the CNCs-RSs. It showed the result of -3.1 mV for the zeta potential of RSs. The negative charge of RSs appears because of the deacylation of RSs in the polar solvents, such as pure water.³³ Based on the abovementioned results, the hydrogen bonds are the possible bonding of the CNCs and RSs, leading to the formation of the CNCs-RSs. Besides the zeta potential, the particle sizes of CNCs and CNCs-RSs were also measured using a particle size analyzer, where the length of CNCs was around 138.8 nm and then became 257.7 nm after modification.

The modification of CNCs using RSs was investigated based on the amount of RSs linked on the CNCs (q) for each combined parameter. The q values obtained are presented in Figure 2. It showed that the highest q value was obtained at the

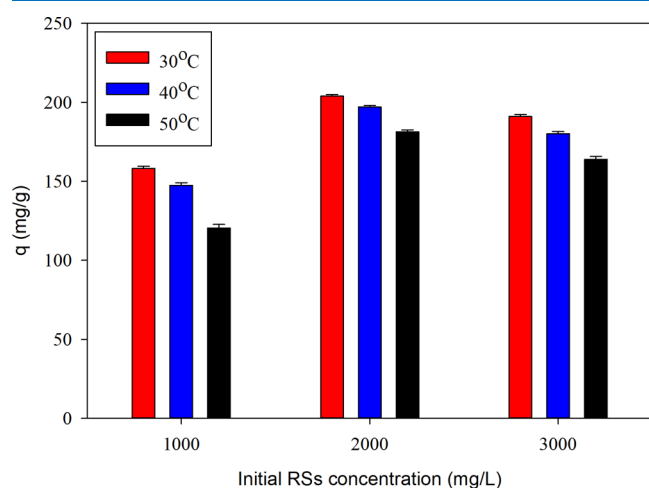


Figure 2. Amounts of RSs linked on the CNCs (q) at combined parameters.

initial RS concentration of 2000 mg/L and the operating temperature of 30 °C, among all of the combined parameters used. The increase in the operating temperature generates low amounts of RSs linked on the CNCs. It is due to the termination of the hydrogen bonds at the operating temperature rise. The hydrogen bonds of crystalline materials have a low strength on the heating process.³⁵ Moreover, the initial RS concentration becomes an important parameter to form the CNCs-RSs. From 1000 to 2000 mg/L of initial RS concentrations, the q value showed an increase in the amounts because of the rich OH groups on the surface of both materials that trigger the formation of the hydrogen bonds. However, the q value decreased along with the increase in the initial RS concentration above 2000 mg/L. At the high initial RS concentration, the negative charges of RSs will increase and inhibit the formation of the CNCs-RSs. It is caused by the repulsion of the CNCs and RSs where both have negative charges. The 2000 mg/L of initial RS concentration becomes the highest limit to form the optimum CNCs-RSs. The highest q value obtained was 203.81 ± 0.98 mg/g. It is higher than the modification of CNCs using several previous modification agents, such as CTAB (115.21 mg/g)¹ and fatty acid methyl ester ($12.5 \pm 1.2\%$ or around 125 mg/g).¹⁵

Scanning electron microscopy (SEM) images figure out the morphology of CNCs, RSs, and CNCs-RSs, as shown in Figure 3. The CNCs have a rod-like structure that is connected to each other, as depicted in Figure 3i. Meanwhile, the RS morphology (Figure 3ii) shows the chunks of the RS agglomeration. The RS agglomeration is possibly caused by the presence of the hydrophobic regions of the RS when inside a polar solvent. The morphology of CNCs-RSs is shown in Figure 3iii. The CNCs unravel into single rod-like structures and are coated by the RS compound. This morphology of CNCs-RSs is advantageous as a drug carrier because of the increase in the active sites for binding the drugs. There has been no comparison before this investigation of CNCs-RSs.

The X-ray Diffraction (XRD) spectra (Figure 4) show that the modification using RSs does not shift the curve of the

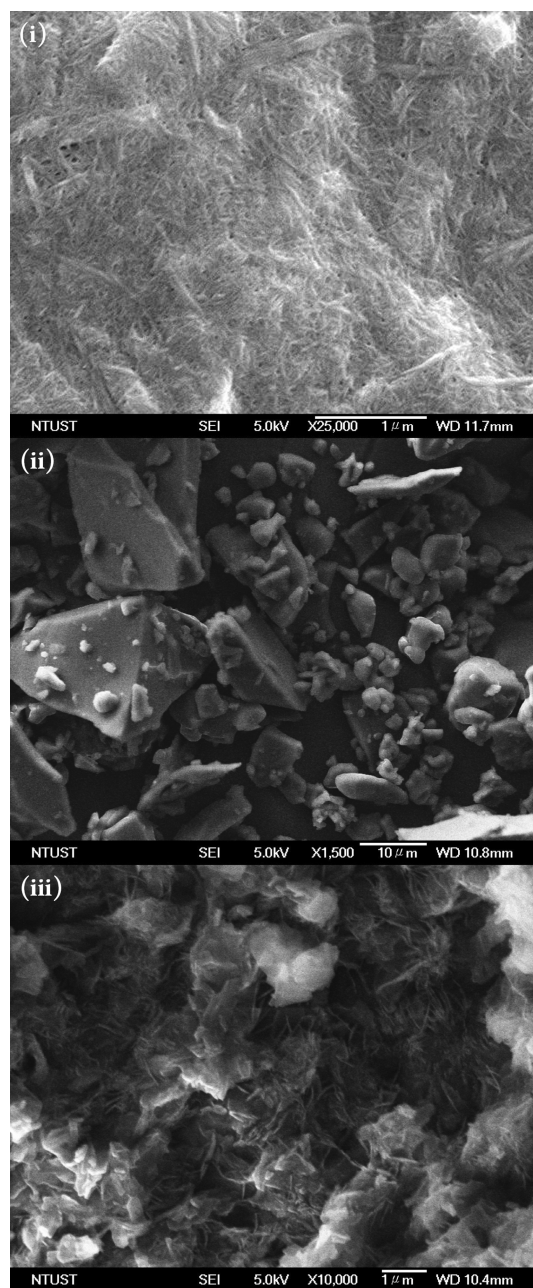


Figure 3. SEM images of CNCs (i), RSs (ii), and CNCs-RSs (iii).

original CNCs. In other words, the modification process does not change the structure and shape of the CNCs. The CrIs of CNCs and CNCs-RSs were presented by the peaks at 2θ of 15.5° (110), 16.4° (110), 22.8° (200), and 35° (004) as compared to the cellulose I crystal standard (JCPDS no. 00-050-22411). However, the CrI of the CNCs-RSs decreased slightly compared to the original CNCs. The results show that the CrI of CNCs and CNCs-RSs was 82.69 and 77.19%, respectively. It is due to the presence of the amorphous structure of the RSs on the CNC surface.

Figure 5 shows the Fourier transform infrared (FTIR) spectra of the CNCs and CNCs-RSs to confirm the transformation of the chemical groups. The presence of sulfate groups on the CNC surface is proven by the appearance of the S=O vibration peak at 1253.6 cm^{-1} .³² This causes the CNCs to have a negative charge, as shown in the zeta potential result.

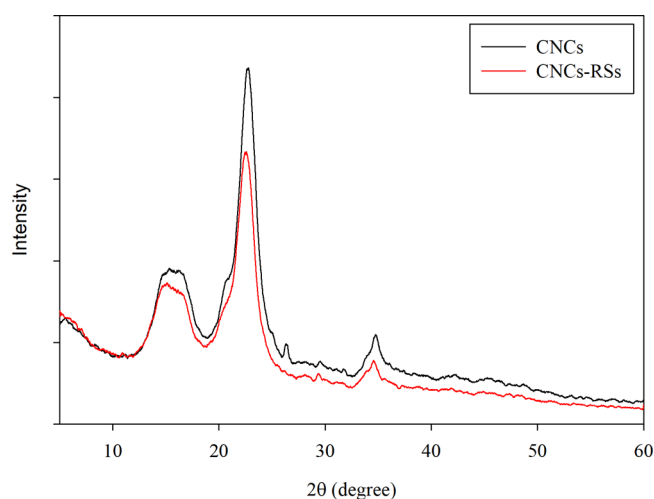


Figure 4. XRD spectra of CNCs and CNCs-RSs.

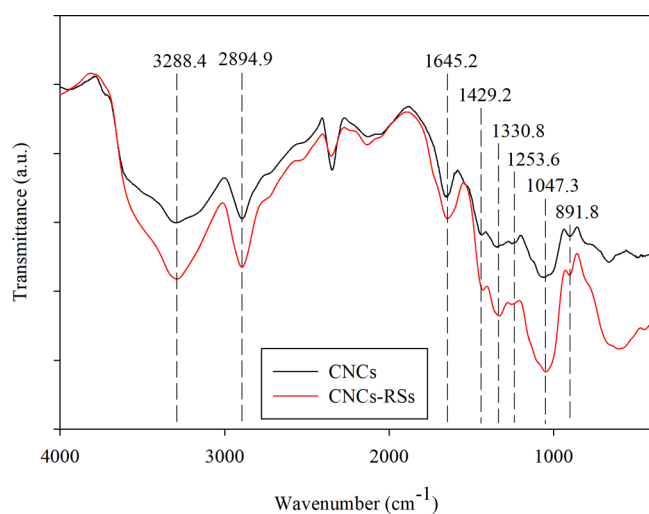


Figure 5. FTIR spectra of CNCs and CNCs-RSs.

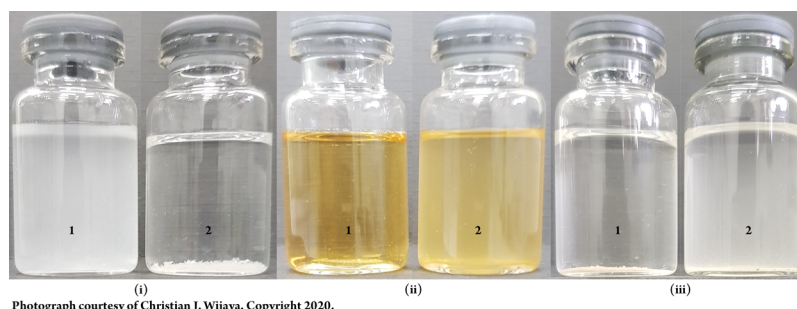
Because of the significant difference of the OH stretching peak at 3288.4 cm^{-1} between CNC and CNCs-RS spectra,³⁶ the OH functional groups on the CNC and RS surfaces involved in the bonding of CNCs-RSs. This result shows a similar phenomenon with the previous study,²⁷ where the RSs are attached onto the CNCs through the OH functional groups on the surfaces. The aglycone region of RSs is presented in the CNCs-RS spectra, as shown by the peak of olefin functional groups at 1645.2 cm^{-1} .³³ Meanwhile, the oligosaccharide region of RSs is indicated by the increase in several peaks, such

as at 2894.9 cm^{-1} (C–H stretching), 1429.2 cm^{-1} (C–H bending), 1330.8 cm^{-1} (CH_2 bonding at C_6 of glucose), 1047.3 cm^{-1} (CO stretching), and 891.8 cm^{-1} (β -glycosidic linkages).³⁷ The presence of several functional groups from aglycone and oligosaccharide regions of RSs proves that the RSs are well-attached to the CNCs to form the CNCs-RSs.

Figure 6 shows the dispersing CNCs, RSs, and CNCs-RSs in two kinds of solvents, that is, water as the polar solvent and tetrahydrofuran (THF) as the nonpolar solvent. The polarity indexes of water and THF are 10.2 and 4.0, respectively. The CNCs were wholly dispersed in water, while they were suspended in THF, as shown in Figure 6A. It proves the hydrophilicity of the CNCs that have a water-stable characteristic. The water-stable characteristic was stated because of the negative charge on the CNC surface.³⁸ The RSs are a natural surfactant that has both hydrophilic and hydrophobic characteristics, as shown in Figure 6B. The RSs were dispersed in both water and THF. Moreover, the RSs were dissolved in water as shown as the clear RS solution. However, the hazy RS solution in THF exhibits the hydrophobicity of the RSs. As a result of this modification process, the CNCs-RSs have a hydrophobic characteristic, as shown in Figure 6C where the CNCs-RSs were dispersed in THF. The deposit of CNCs-RSs in water indicates that these have very low hydrophilicity. It shows the significant effects of the RSs linked on the surface of the CNCs. Based on these dispersion characteristics, this modification process using the RSs is successfully used to convert hydrophilic CNCs to hydrophobic CNCs-RSs.

The modification process using the RSs toward the CNCs is a promising process to generate the hydrophobic nanoparticles compared to the previous research studies. The use of RSs is more environmentally friendly and safer for human health than the previous modification agents that have several negative impacts on their excessive exposure to the environment and the human body. Besides that, the RSs are easier to be obtained and isolated from several abundant natural resources. The CNCs-RSs are a potential drug carrier for hydrophobic drugs in the medical fields.

2.3. Analysis of Variance (ANOVA). Statistical verification was carried out using two-way ANOVA with interaction using Minitab 16 statistical software (Minitab Inc., ITS Surabaya, Indonesia). It is used to identify the significances of both independent variables (the initial RS concentrations and the operating temperatures) and their interaction. It used a full factorial design for obtaining the data, where the data were obtained by combining two variables having three levels in each variable. The experiments were conducted in three replications.



Photograph courtesy of Christian J. Wijaya. Copyright 2020.

Figure 6. Visualization of CNCs (i), RSs (ii), and CNCs-RSs (iii) dispersion characteristics (0.1 wt %) in water (1) and THF (2).

Table 1. Results of ANOVA Analysis^a

source	degree of freedom (DF)	sum of squares (SS)	mean squares (MS)	F-value	p-value	contribution (%)
A	2	3977.1	1988.54	870.82	0.000	23.31
B	2	12,832.5	6416.27	2809.81	0.000	75.20
A × B	4	213.0	53.24	23.31	0.000	1.25
error	18	41.1	2.28			0.24
total	26	17,063.7				100

^aS = 1.511; R² = 99.76%; and R² (adj) = 99.65%.

The Fisher values (*F*-values) show the significances of both independent variables and their interaction was higher than their minimum value of the *F*. Furthermore, the significances were also proven by the probability values (*p*-values) where it should be lower than 5%. According to the *F*-values and *p*-values (Table 1), both independent variables and their interaction indicate significant impacts on the amount of RSs linked on the CNCs (*q*). Based on the contribution values, the initial RS concentration has a large effect on *q* compared to the other variables, as shown from the contribution value of 75.20%. This two-way ANOVA with interaction fits these data well as proven by the quiet low standard deviation (*S*) and high *R*-squared (R²).

2.4. Curcumin Uptake on CNCs-RSs. The hydrophobicity enhancement of CNCs using RS modification was aimed to deliver a hydrophobic drug into the human body. Figure 7 shows the uptake and uptake efficiency of curcumin on the CNCs-RSs, which increase along with the interval time used. The CNCs-RS mass to curcumin solution volume ratio (*R*) of 1:5 mg/mL shows higher uptake than the *R* of 1:1 mg/mL, as shown in Figure 7i, which reached 12.40 ± 0.24% at 600 min. This occurred because of the high solvent volume used in the use of *R* = 1:5 mg/mL, which lower the randomness in the solid–solution interface. The lower randomness induced the high and strong binding of CNCs-RSs and curcumin. On the contrary, the uptake efficiency was lower in the use of *R* = 1:5 mg/mL, as shown in Figure 7ii, which reached 49.49 ± 0.94%. Because of the high curcumin amounts contained in the solution, CNCs-RSs could not load all of the curcumin amounts from the curcumin solution. As compared to the previous study, the uptake of tetracycline on the CNCs-RSs just reached 18.11 μg/mg or around 1.81%,²⁷ while the uptake of curcumin using CNCs-CTAB was 57.6 μg/mg or around 5.76% (the binding efficiency up to 96%).³ CNCs-RSs had a higher uptake of curcumin because of their hydrophobic characteristic. Other than that, CNCs-RSs can exceed the curcumin uptake of CNCs-CTAB which have a tendency and possibility to cause health and environmental issues. These proved that the modification of CNCs using RSs was successfully carried out to enhance their hydrophobicity. RSs have aglycone (more hydrophobic) and oligosaccharide (more hydrophilic) sides, as shown in Figure 8i. The curcumin which has hydrophobic characteristic (Figure 8ii) was attracted on the aglycone side of RSs.

2.5. Curcumin Release from CNCs-RSs. The release experiment used curcumin-loaded CNCs-RSs from the curcumin uptake experiment at the highest curcumin uptake. The release of curcumin from CNCs-RSs showed a slow-release mechanism in the medium with pH 7.4, as shown in Figure 9. Only approximately 43% of curcumin was released in a day and then became approximately 78% in 3 days. This was very beneficial because the release of the drug could be controlled slowly. Moreover, the curcumin could be released

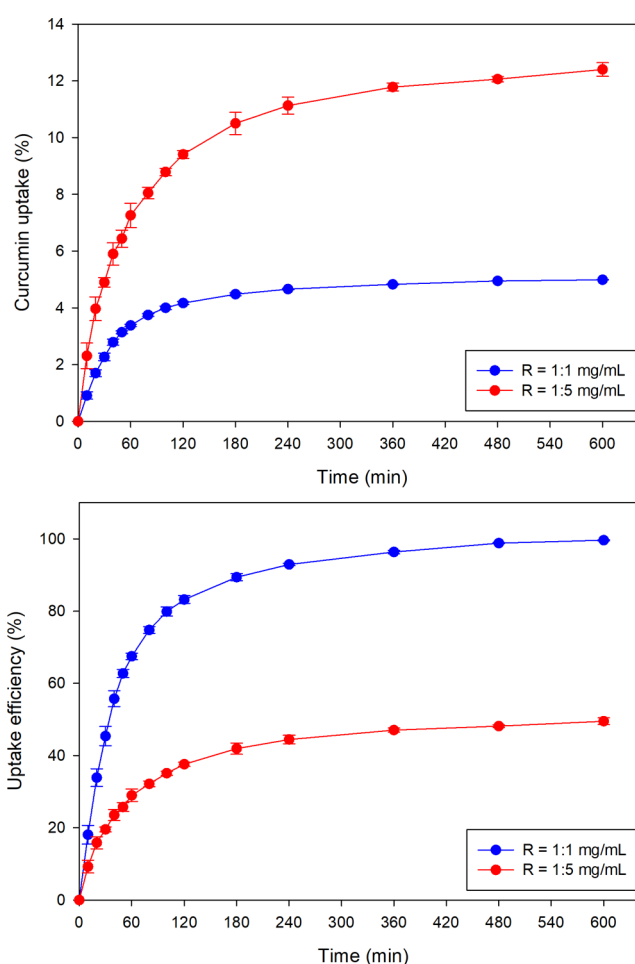


Figure 7. Uptake (i) and uptake efficiency (ii) of curcumin on the CNCs-RSs.

well in the medium with pH 7.4, where pH 7.4 is the pH of ileum in the human body. The curcumin-loaded CNCs-RSs were good for targeting a release in the ileum. However, it still needs further investigations.

3. CONCLUSIONS

The modification of CNCs using RSs was successfully carried out to enhance the hydrophobicity of CNCs. The RSs were well-attached onto the CNCs, as shown in the FTIR analysis. The CNCs-RSs could be dispersed in a nonpolar solvent such as THF that indicates the high hydrophobicity enhancement. These are promising advanced materials for hydrophobic drug carriers. Because these are composed of a cellulose-based material and natural surfactant, they are safe for humans and the environment. Although, the cytotoxicity must be examined further in the future. The highest amount of RSs linked on the CNCs reached 203.81 ± 0.98 mg/g that are attached by

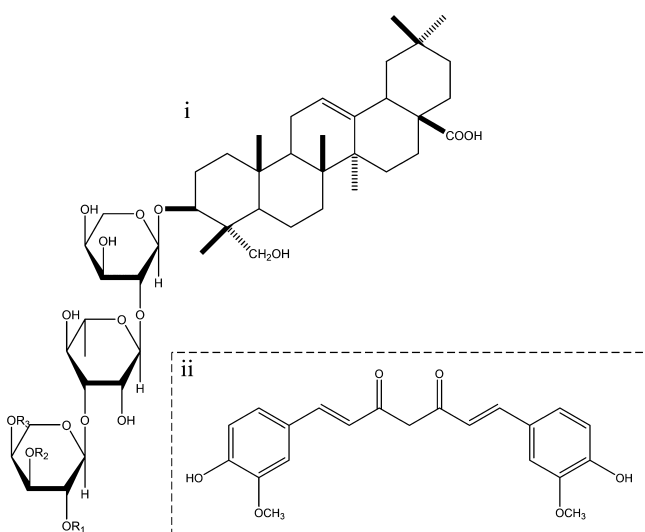


Figure 8. Chemical structures of RSs (i) and curcumin (ii).

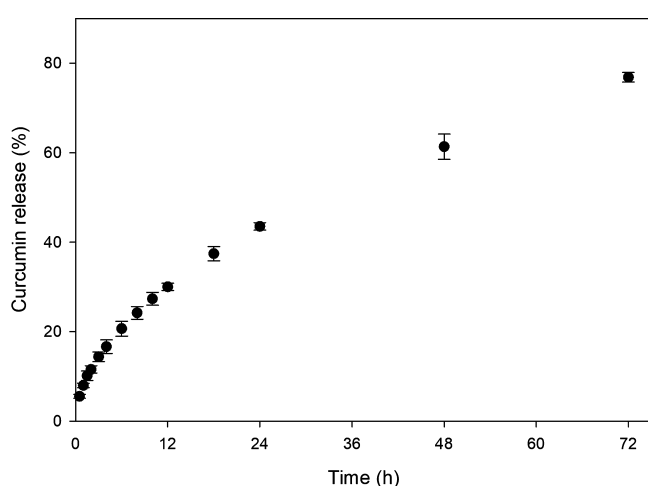


Figure 9. Accumulative release of curcumin from curcumin-loaded CNCs-RSs.

hydrogen bonds, as shown by the FTIR analysis. The modification process is significantly affected by the initial RS concentration and operating temperature as proven by the ANOVA analysis, where both variables indicate the p -value of less than 5%. Two-way ANOVA with interaction fitted the experimental data well.

4. EXPERIMENTAL SECTION

4.1. Materials. *Dendrocalamus asper*-type BSs were collected from the traditional market in Surabaya, East Java, Indonesia. The flesh fruits of the *S. rarak De Candolle* plant were collected from the wild plants in Malang, East Java, Indonesia. Both natural resources were dried under sunlight and pounded to powder. All chemicals, that is, sodium hydroxide, hydrogen peroxide (50%), sulfuric acid (95–98%), ethanol (96%), and tetrahydrofuran ($\geq 99\%$), were purchased from Sigma-Aldrich (Singapore) in analytical grade.

4.2. Preparation of CNCs. CNCs were prepared using the previously established method.³⁹ A total of 10 g of BS powder was added into 200 mL of sodium hydroxide solution 20% (w/v) while the solution was heated at 90 °C and kept for 4 h under stirring. Then, it was continued by the bleaching process

using 25 mL of sodium hydroxide solution 4% (w/v) at 50 °C while the same amounts of hydrogen peroxide 50% were added dropwise. It is continued for 60 min under stirring. At the end of each step, the residue was dried at 50 °C and collected for the next processes. The product of this stage was the PBSs that contained high cellulose content.

The acid hydrolysis process was conducted to produce CNCs from PBSs. The optimum condition from the previous study was applied in this study to obtain a consistent product.³⁹ PBSs were hydrolyzed using sulfuric acid solution 55 wt % with a PBS mass to sulfuric acid solution ratio of 1:20 at 40 °C for 60 min. To stop the hydrolysis process, 10-fold cold-distilled water was poured into the solution. The suspension was centrifuged to remove the acid solution and dialyzed using distilled water until neutral pH was reached. Then, it was sonicated for 20 min. The final suspension was dried using a freeze dryer at a pressure of 0.08 mbar and a temperature of -42 °C. The final product of this stage was the CNCs and they were used for the modification process.

4.3. Extraction of RSs. *S. rarak De Candolle* is a wild plant that is widely populated in South East Asia, especially, Indonesia. The extraction process followed the previously established method with a slight adjustment.^{27,33} The powdered fruit fleshes (15 g) were extracted using 200 mL of distilled water at 80 °C for 60 min. The supernatant was obtained by removing the solid residue using centrifugation at 4000 rpm for 10 min. The supernatant was dried using a freeze dryer at a pressure of 0.08 mbar and a temperature of -42 °C.

4.4. Surface Modification of CNCs. The CNC suspension in water (0.25 wt %) was added into 100 mL of the RS solution with various initial concentrations (1000, 2000, and 3000 mg/L). The mixture was conditioned under various operating temperatures (30, 40, and 50 °C) for 3 h. Then, the process was continued until 24 h under room temperature. These consecutive processes were carried out under gentle stirring. The modified CNCs were washed using centrifugation at 6000 rpm for 10 min (3 times) to remove the excess RSs. The final suspension was dried using a freeze dryer at a pressure of 0.08 mbar and a temperature of -42 °C to obtain the dried CNCs-RSs.

The modification of CNCs-RSs was conducted under various combined conditions: the initial RS concentrations (1000, 2000, and 3000 mg/L) and the operating temperatures (30, 40, and 50 °C), leading to nine experimental combinations with three replications. These various combined variables were used to investigate the effects of both variables toward the binding of CNCs-RSs.

4.5. Identifications and Characterizations. **4.5.1. Determination of Total Saponin Content.** A calibration curve was prepared by varying the concentration of diosgenin solution as the standard solution (100–700 mg/L). The diosgenin was dissolved in the aqueous methanol 80%. A total of 0.25 mL of the diosgenin solution was added to 0.25 mL of the vanillin reagent (8% in ethanol) and 2.5 mL of sulfuric acid 72% (v/v), respectively. The mixture was heated at 60 °C in a water bath for 10 min and cooled in an ice bath for 3 min. The absorbance was measured using a UV/vis spectrophotometer at 544 nm against the blank solution (diosgenin solution 0 mg/L). For the sample measurement, the sample solution replaced the diosgenin solution and was treated the same as the standard measurement (Figure 10).

The calibration curve of this determination was linearized using the following equation

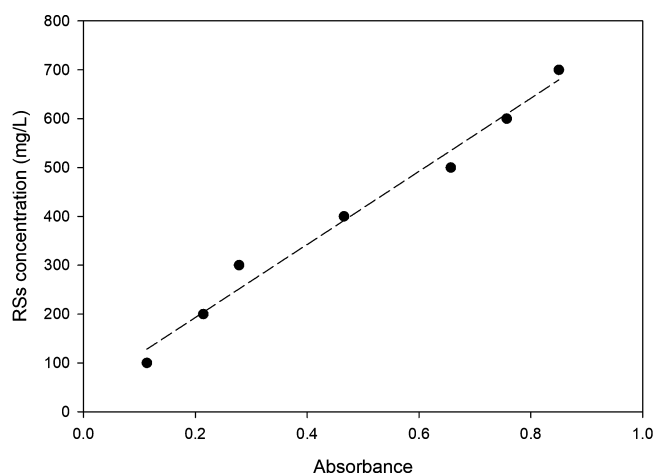


Figure 10. Calibration curve of RS concentration.

$$[RS] = 43.34 + 748.59Abs \quad (1)$$

where Abs is the absorbance value of the sample while [RS] is the concentration of the RS sample.

4.5.2. Determination of RS Amounts in the CNCs-RSs. To know the amounts of RSs linked on the CNCs, the RS concentration in the initial and residual solution of the modification process was determined using a UV/vis spectrophotometer as explained before. The amounts of RSs linked on the CNCs were expressed as q (mg/g) using the following equation¹

$$q = [(C_o - C_e)/m] \times V \quad (2)$$

where C_o and C_e (mg/L) are the initial and equilibrium concentrations of the RS solution, respectively. V (L) is the total volume of the solution in the modification process, while m (g) is the mass of the CNCs used.

4.5.3. Zeta Potential and Particle Size Analysis. This measurement was conducted for the zeta potentials of CNCs and RSs and the particle sizes of the CNCs and CNCs-RSs using a Zeta sizer Nano series, Malvern Instrument. The samples were suspended in distilled water with a concentration of 0.1 wt %. This analysis was used to investigate the zeta potential and particle size of each sample for knowing the possible interaction and change between these two constituents of the CNCs-RSs. The measurement results were expressed as the average value of five measurements.

4.5.4. XRD Analysis. The X-ray diffractograms of the CNCs and CNCs-RSs were obtained from the XRD analysis using a PANalytical X'Pert PRO X-ray diffractometer with a monochromated high-intensity Cu $K\alpha$ radiation (1.5406 Å) operating at 40 kV and 30 mA. It was conducted using a step size of $0.02^\circ/C$ in the angle range of $5-60^\circ$. The CrI was determined using the Segal's equation¹⁸

$$CrI = [(I_{002} - I_{am})/I_{002}] \times 100\% \quad (3)$$

where I_{am} represents the minimum intensity between 110 and 200 lattice diffractions which indicates the amorphous region, while I_{002} is the intensity of the 002 lattice peak which indicates the total amorphous and crystalline regions.

4.5.5. Scanning Electron Microscopy Analysis. The morphologies of the CNCs, RSs, and CNCs-RSs were observed by the SEM analysis. A thin layer of conductive platinum was used to coat the samples in an argon atmosphere

using a JFC-1200 coater, JEOL, Ltd., Japan. The SEM analysis was conducted using a JEOL JSM-6390 field emission SEM.

4.5.6. Fourier Transform Infrared Spectroscopy Analysis. The comparisons between the CNC, RS, and CNCs-RS functional groups were carried out by the FTIR analysis using FTIR Shimadzu 8400S. The KBr pelleting method was used to analyze the samples. The analysis was conducted in the wavenumber range of $4000-400\text{ cm}^{-1}$. The functional group analysis can indicate the interaction between the CNCs and RSs, leading to the formation of the CNCs-RSs.

4.5.7. Dispersion Characteristic Analysis. The CNC, RS, and CNCs-RS samples (0.1 wt %) were dispersed in polar (water) and nonpolar (THF) solvents using sonication for 1 h. Then, the suspensions were left for 3 weeks at room temperature. The dispersion characteristic investigation was carried out under the final condition of the suspensions.

4.6. Statistics. Two-way ANOVA with interaction was conducted to investigate the significances of the chosen parameters in the modification process using a significance level (α) of 0.05. The data represent the average of three repetitions for each combined parameter.

4.7. Curcumin Uptake. Batch adsorption was carried out to investigate the curcumin uptake on CNCs-RSs. CNCs-RSs were added to the curcumin-ethanol solution (50 mg/L) with a CNCs-RS mass to curcumin solution volume ratio (R) of 1:1 and 1:5 mg/mL. The solutions were shaken using a thermostatic shaking water bath (Mettler type WB-14) at 30°C for varied interval time (0–600 min). After loading, the curcumin-loaded CNCs-RSs were separated from the solution by centrifugation. The remaining curcumin in solutions was measured using a UV/vis spectrophotometer at a maximum wavelength of 430 nm. The uptake (U) and uptake efficiency (UE) percentages of curcumin on the CNCs-RSs were calculated according to the equations given below⁴⁰

$$U = [(m_{i-cur} - m_{r-cur})/m_{CNCs-RSs}] \times 100\% \quad (4)$$

$$UE = [(m_{i-cur} - m_{r-cur})/m_{i-cur}] \times 100\% \quad (5)$$

where m_{i-cur} is the mass of the initial curcumin added in the solution, m_{r-cur} is the mass of the remaining curcumin in the solution, and $m_{CNCs-RSs}$ is the mass of CNCs-RSs used. The experiment of curcumin uptake was carried out with three replications.

4.8. Curcumin Release. Loaded curcumin was released from CNCs-RSs by soaking 50 mg of curcumin-loaded CNCs-RSs in 50 mL of phosphate-buffered solution (pH 7.4). The solutions were shaken using a thermostatic shaking water bath at 37°C for varied interval time (0–72 h). The solid was removed from the solution by centrifugation. The released curcumin in the solution was measured using a UV/vis spectrophotometer at 430 nm. The experiment of curcumin release was carried out with three replications.

AUTHOR INFORMATION

Corresponding Author

Setiyo Gunawan – Department of Chemical Engineering, Faculty of Industrial Technology, Institut Teknologi Sepuluh Nopember, Surabaya 60111, Indonesia; orcid.org/0000-0003-4864-4465; Phone: +62-31-5946240; Email: gunawan@chem-eng.its.ac.id; Fax: +62-31-5999282

Authors

Christian J. Wijaya – Department of Chemical Engineering, Faculty of Industrial Technology, Institut Teknologi Sepuluh Nopember, Surabaya 60111, Indonesia; Department of Chemical Engineering, Widya Mandala Surabaya Catholic University, Surabaya 60114, Indonesia

Suryadi Ismadji – Department of Chemical Engineering, Widya Mandala Surabaya Catholic University, Surabaya 60114, Indonesia; Department of Chemical Engineering, National Taiwan University of Science and Technology, Taipei 10607, Taiwan

Hakun W. Aparamarta – Department of Chemical Engineering, Faculty of Industrial Technology, Institut Teknologi Sepuluh Nopember, Surabaya 60111, Indonesia

Complete contact information is available at:

<https://pubs.acs.org/10.1021/acsoomega.0c02425>

Author Contributions

The manuscript was written through contributions of all the authors. All the authors have given approval to the final version of the manuscript.

Notes

The authors declare no competing financial interest.

ACKNOWLEDGMENTS

The authors thank the Directorate General of Resources for Science, Technology, and Higher Education, Ministry of Research, Technology, and Higher Education of Republic Indonesia (no. 1116/PKS/ITS/2020) and Widya Mandala Surabaya Catholic University for the financial support in this research.

REFERENCES

- (1) Qing, W.; Wang, Y.; Wang, Y.; Zhao, D.; Liu, X.; Zhu, J. The modified nanocrystalline cellulose for hydrophobic drug delivery. *Appl. Surf. Sci.* **2016**, *366*, 404–409.
- (2) Shang, Q.; Liu, C.; Hu, Y.; Jia, P.; Hu, L.; Zhou, Y. Bio-inspired hydrophobic modification of cellulose nanocrystals with castor oil. *Carbohydr. Polym.* **2018**, *191*, 168–175.
- (3) Zainuddin, N.; Ahmad, I.; Kargarzadeh, H.; Ramli, S. Hydrophobic kenaf nanocrystalline cellulose for the binding of curcumin. *Carbohydr. Polym.* **2017**, *163*, 261–269.
- (4) Lin, N.; Huang, J.; Chang, P. R.; Feng, J.; Yu, J. Surface acetylation of cellulose nanocrystal and its reinforcing function in poly(lactic acid). *Carbohydr. Polym.* **2011**, *83*, 1834–1842.
- (5) Kaboorani, A.; Riedl, B. Surface modification of cellulose nanocrystals (CNC) by a cationic surfactant. *Ind. Crops Prod.* **2015**, *65*, 45–55.
- (6) Supramaniam, J.; Adnan, R.; Mohd Kaus, N. H.; Bushra, R.; Bushra, R. Magnetic nanocellulose alginate hydrogel beads as potential drug delivery system. *Int. J. Biol. Macromol.* **2018**, *118*, 640–648.
- (7) Mauricio, M. R.; da Costa, P. G.; Haraguchi, S. K.; Guilherme, M. R.; Muniz, E. C.; Rubira, A. F. Synthesis of a microhydrogel composite from cellulose nanowhiskers and starch for drug delivery. *Carbohydr. Polym.* **2015**, *115*, 715–722.
- (8) Wijaya, C. J.; Saputra, S. N.; Soetaredjo, F. E.; Putro, J. N.; Lin, C. X.; Kurniawan, A.; Ju, Y.-H.; Ismadji, S. Cellulose nanocrystals from passion fruit peels waste as antibiotic drug carrier. *Carbohydr. Polym.* **2017**, *175*, 370–376.
- (9) Letchford, K.; Jackson, J. K.; Wasserman, B. Z.; Ye, L.; Hamad, W. Y.; Burt, H. M. The use of nanocrystalline cellulose for the binding and controlled release of drugs. *Int. J. Nanomed.* **2011**, *6*, 321–330.
- (10) Taheri, A.; Mohammadi, M. The use of cellulose nanocrystals for potential application in topical delivery of hydroquinone. *Chem. Biol. Drug Des.* **2015**, *86*, 102–106.
- (11) Ooi, S. Y.; Ahmad, I.; Amin, M. C. I. M. Cellulose nanocrystals extracted from rice husks as a reinforcing material in gelatin hydrogels for use in controlled drug delivery systems. *Ind. Crops Prod.* **2016**, *93*, 227–234.
- (12) Cheng, Q.; Ye, D.; Chang, C.; Zhang, L. Facile fabrication of superhydrophilic membranes consisted of fibrous tunicate cellulose nanocrystals for highly efficient oil/water separation. *J. Membr. Sci.* **2017**, *525*, 1–8.
- (13) Cao, L.; Huang, J.; Chen, Y. Dual cross-linked epoxidized natural rubber reinforced by tunicate cellulose nanocrystals with improved strength and extensibility. *ACS Sustainable Chem. Eng.* **2018**, *6*, 14802–14811.
- (14) Yoo, Y.; Youngblood, J. P. Green one-pot synthesis of surface hydrophobized cellulose nanocrystals in aqueous medium. *ACS Sustainable Chem. Eng.* **2016**, *4*, 3927–3938.
- (15) Wei, L.; Agarwal, U. P.; Hirth, K. C.; Matuana, L. M.; Sabo, R. C.; Stark, N. M. Chemical modification of nanocellulose with canola oil fatty acid methyl ester. *Carbohydr. Polym.* **2017**, *169*, 108–116.
- (16) Dong, S.; Cho, H. J.; Lee, Y. W.; Roman, M.; Tech, V.; States, U. Synthesis and cellular uptake of folic acid-conjugated cellulose nanocrystals for cancer targeting. *Biomacromolecules* **2014**, *15*, 1560–1567.
- (17) Ndong Ntoutoume, G. M. A.; Granet, R.; Mbakidi, J. P.; Brégier, F.; Léger, D. Y.; Fidanzi-Dugas, C.; Lequart, V.; Joly, N.; Liagre, B.; Chaleix, V.; et al. Development of curcumin–cyclodextrin/cellulose nanocrystals complexes: New anticancer drug delivery systems. *Bioorg. Med. Chem. Lett.* **2016**, *26*, 941–945.
- (18) Chen, Q.-H.; Zheng, J.; Xu, Y.-T.; Yin, S.-W.; Liu, F.; Tang, C.-H. Surface modification improves fabrication of pickering high internal phase emulsions stabilized by cellulose nanocrystals. *Food Hydrocolloids* **2018**, *75*, 125–130.
- (19) Rescignano, N.; Fortunati, E.; Armentano, I.; Hernandez, R.; Mijangos, C.; Pasquino, R.; Kenny, J. M. Use of alginate, chitosan and cellulose nanocrystals as emulsion stabilizers in the synthesis of biodegradable polymeric nanoparticles. *J. Colloid Interface Sci.* **2015**, *445*, 31–39.
- (20) Akhlaghi, S. P.; Berry, R. C.; Tam, K. C. Surface modification of cellulose nanocrystal with chitosan oligosaccharide for drug delivery applications. *Cellulose* **2013**, *20*, 1747–1764.
- (21) Akhlaghi, S. P.; Berry, R. M.; Tam, K. C. Modified cellulose nanocrystal for vitamin C delivery. *AAPS PharmSciTech* **2014**, *16*, 306–314.
- (22) Mohanta, V.; Madras, G.; Patil, S. Layer-by-layer assembled thin films and microcapsules of nanocrystalline cellulose for hydrophobic drug delivery. *ACS Appl. Mater. Interfaces* **2014**, *6*, 20093–20101.
- (23) Abo-elseoud, W. S.; Hassan, M. L.; Sabaa, M. W.; Basha, M.; Hassan, E. A.; Fadel, S. M. Chitosan nanoparticles/cellulose nanocrystals nanocomposites as a carrier system for the controlled release of repaglinide. *Int. J. Biol. Macromol.* **2018**, *111*, 604–613.
- (24) Rehman, N.; Miranda, C. I. D.; de Miranda, M. I. G.; Rosa, S. M. L. Dynamics of cellulose nanocrystals in the presence of hexadecyltrimethylammonium bromide. *Macromol. Res.* **2017**, *25*, 767–771.
- (25) Seabra, A. B.; Bernardes, J. S.; Fávoro, W. J.; Paula, A. J.; Durán, N. Cellulose nanocrystals as carriers in medicine and their toxicities: A review. *Carbohydr. Polym.* **2018**, *181*, 514–527.
- (26) Vinarov, Z.; Radeva, D.; Katev, V.; Tcholakova, S.; Denkov, N. Solubilisation of hydrophobic drugs by saponins. *Indian J. Pharm. Sci.* **2018**, *80*, 709–718.
- (27) Bundjaja, V.; Sari, T. M.; Soetaredjo, F. E.; Yuliana, M.; Angkawijaya, A. E.; Ismadji, S.; Cheng, K.-C.; Santoso, S. P. Aqueous sorption of tetracycline using rarasaponin-modified nanocrystalline cellulose. *J. Mol. Liq.* **2020**, *301*, 112433.
- (28) Chang, J.; Shen, Z.; Hu, X.; Schulman, E.; Cui, C.; Guo, Q.; Tian, H. Adsorption of tetracycline by shrimp shell waste from

aqueous solutions: Adsorption isotherm, kinetics modeling, and mechanism. *ACS Omega* **2020**, *5*, 3467–3477.

(29) Datta, R. Acidogenic digestion of lignocellulose-acid yield and conversion of components. *Biotechnol. Bioeng.* **1981**, *23*, 2167–2170.

(30) Collazo-bigliardi, S.; Ortega-toro, R.; Chiralt Boix, A. Isolation and characterisation of microcrystalline cellulose and cellulose nanocrystals from coffee husk and comparative study with rice husk. *Carbohydr. Polym.* **2018**, *191*, 205–215.

(31) Ilyas, R. A.; Sapuan, S. M.; Ishak, M. R. Isolation and characterization of nanocrystalline cellulose from sugar palm fibres (*Arenga pinnata*). *Carbohydr. Polym.* **2018**, *181*, 1038–1051.

(32) Gu, J.; Hu, C.; Zhong, R.; Tu, D.; Yun, H.; Zhang, W.; Leu, S.-Y. Isolation of cellulose nanocrystals from medium density fiberboards. *Carbohydr. Polym.* **2017**, *167*, 70–78.

(33) Kurniawan, A.; Sutiono, H.; Ju, Y.-H.; Soetaredjo, F. E.; Ayucitra, A.; Yudha, A.; Ismadji, S. Utilization of rarasaponin natural surfactant for organo-bentonite preparation: Application for methylene blue removal from aqueous effluent. *Microporous Mesoporous Mater.* **2011**, *142*, 184–193.

(34) Ditzel, F. I.; Prestes, E.; Carvalho, B. M.; Demiate, I. M.; Pinheiro, L. A. Nanocrystalline cellulose extracted from pine wood and corncob. *Carbohydr. Polym.* **2017**, *157*, 1577–1585.

(35) Tang, X. C.; Pikal, M. J.; Taylor, L. S. The effect of temperature on hydrogen bonding in crystalline and amorphous phases in dihydropyridine calcium channel blockers. *Pharm. Res.* **2002**, *19*, 484–490.

(36) Hernandez, C. C.; Ferreira, F. F.; Rosa, D. S. X-ray powder diffraction and other analyses of cellulose nanocrystals obtained from corn straw by chemical treatments. *Carbohydr. Polym.* **2018**, *193*, 39–44.

(37) Naduparambath, S.; T.V., J.; V., S.; M.P., S.; Balan, A. K.; E., P. Isolation and characterisation of cellulose nanocrystals from sago seed shells. *Carbohydr. Polym.* **2018**, *180*, 13–20.

(38) Nascimento, D. M.; Almeida, J. S.; Dias, A. F.; Figueirêdo, M. C. B.; Morais, J. P. S.; Feitosa, J. P. A.; Rosa, M. D. F. A novel green approach for the preparation of cellulose nanowhiskers from white coir. *Carbohydr. Polym.* **2014**, *110*, 456–463.

(39) Wijaya, C. J.; Ismadji, S.; Aparamarta, H. W.; Gunawan, S. Optimization of cellulose nanocrystals from bamboo shoots using response surface methodology. *Heliyon* **2019**, *5*, No. e02807.

(40) Zainal-Abidin, M. H.; Hayyan, M.; Ngoh, G. C.; Wong, W. F. Doxorubicin loading on functional graphene as a promising nanocarrier using ternary deep eutectic solvent systems. *ACS Omega* **2020**, *5*, 1656–1668.